

## Covalent and Ionic Nature of the Dative Bond and Account of Accurate Ammonia Borane Binding Enthalpies

Joshua A. Plumley and Jeffrey D. Evanseck\*

Center for Computational Sciences and Department of Chemistry and Biochemistry, Duquesne University, 600 Forbes Avenue, Pittsburgh, Pennsylvania 15282-1530

Received: June 25, 2007; In Final Form: September 14, 2007

The inherent difficulty in modeling the energetic character of the B–N dative bond has been investigated utilizing density functional theory and ab initio methods. The underlying influence of basis set size and functions, thermal corrections, and basis set superposition error (BSSE) on the predicted binding enthalpy of ammonia borane ( $\text{H}_3\text{B}-\text{NH}_3$ ) and four methyl-substituted ammonia trimethylboranes ( $(\text{CH}_3)_3\text{B}-\text{N}(\text{CH}_3)_n\text{H}_{3-n}$ ;  $n = 0-3$ ) has been evaluated and compared with experiment. HF, B3LYP, MPW1K, MP2, QCISD, and QCISD(T) have been utilized with a wide range of Pople and correlation-consistent basis sets, totaling 336 levels of theory. MPW1K, B3LYP, and HF result in less BSSE and converge to binding enthalpies with fewer basis functions than post-SCF techniques; however, the methods fail to model experimental binding enthalpies and trends accurately, producing mean absolute deviations (MADs) of 5.1, 10.8, and 16.3 kcal/mol, respectively. Despite slow convergence, MP2, QCISD, and QCISD(T) using the 6-311++G(3df,2p) basis set reproduce the experimental binding enthalpy trend and result in lower MADs of 2.2, 2.6, and 0.5 kcal/mol, respectively, when corrected for BSSE and a residual convergence error of ca. 1.3–1.6 kcal/mol. Accuracy of the predicted binding enthalpy is linked to correct determination of the bond's dative character given by charge-transfer frustration,  $Q_{\text{CTF}} = -(\Delta Q_{\text{N}} + \Delta Q_{\text{B}})$ . Frustration gauges the incompleteness of charge transfer between the donor and the acceptor. The binding enthalpy across ammonia borane and methylated complexes is correlated to its dative character ( $R^2 = 0.91$ ), where a more dative bond (less charge-transfer frustration) results in a weaker binding enthalpy. However, a balance of electronic and steric factors must be considered to explain trends in experimentally reported binding enthalpies. Dative bond descriptors, such as bond ionicity and covalency are important in the accurate characterization of the dative bond. The B–N dative bond in ammonia borane is 65% ionic, moderately strong ( $-27.5 \pm 0.5$  kcal/mol), and structurally flexible on the donor side to relieve steric congestion.

### Introduction

The dative bond, also known as the coordinate covalent bond,<sup>1,2</sup> semipolar double bond,<sup>3–5</sup> or coordinate link,<sup>6,7</sup> has been less defined and studied as compared to either covalent or ionic bonds.<sup>8–10</sup> Depending upon the field of study, molecular systems with dative bonds are typically referred to as coordination compounds,<sup>11</sup> Lewis acid–base adducts,<sup>12</sup> or electron donor–acceptor complexes.<sup>13–15</sup> Despite the nomenclature, these molecular systems employ an atypical bonding scheme, where covalent and ionic potential energy surfaces become close in energy.<sup>16</sup> The wave function for dative bonding is described as

$$\Psi_{\text{dative}}(\text{D}^+-\text{A}^-) = a\Psi_{\text{covalent}}(\text{D}-\text{A}) + b\Psi_{\text{ionic}}(\text{D}^+,\text{A}^-)$$

The importance of each bonding term depends upon the ability of the atomic partners to share electrons as well as D to donate electrons and A to accept them. It has been reported previously that the B–N bond strength includes contributions from both covalent and ionic terms, making trends in bond energies difficult to predict a priori.<sup>17</sup> Thus, a difficult situation results for the computational treatment of the structure, energetics, and dynamics of the dative bond, because the employed chemical

theory must simultaneously treat the partial covalent and ionic contributions accurately without compensation of errors.

To date, the binding energetics for ammonia borane,  $\text{H}_3\text{B}-\text{NH}_3$ , a well-known prototype of the dative bond,<sup>3</sup> have not been directly measured by experiment. As a result of the computational challenge in modeling both the covalent and the ionic character of the dative bond, the predicted binding energetics vary widely.<sup>3,18–25</sup> Table 1 is a noncomprehensive summary of the predicted binding energetics reported using different levels of theory with and without basis set superposition error (BSSE) and thermal corrections.

To the best of our knowledge, there exists two estimates of the  $\text{H}_3\text{B}-\text{NH}_3$  binding enthalpy derived indirectly from experimental data. The earliest  $\text{H}_3\text{B}-\text{NH}_3$  binding enthalpy was provided by Haaland, extrapolated from the experimental binding enthalpies of seven methylated boranes.<sup>3</sup> The estimation was reproduced (Figure S1 of the Supporting Information) by using a quadratic fit of the plotted binding enthalpies for  $(\text{CH}_3)_3\text{B}-\text{N}(\text{CH}_3)_n\text{H}_{3-n}$ ,  $n = 0-3$ , versus the number of methyl substituents on nitrogen,  $n$ , as done by Brown et al.<sup>26</sup> Subsequently, a second quadratic equation was fitted to the binding enthalpies for  $\text{H}_3\text{B}-\text{N}(\text{CH}_3)_n\text{H}_{3-n}$  versus the same  $x$ -axis. The binding enthalpy of  $\text{H}_3\text{B}-\text{NH}_3$  was taken as the value that allowed the coefficient of the quadratic term within the two equations to be equivalent. Haaland's resulting binding enthalpy

\* Author to whom correspondence should be addressed. E-mail: evanseck@duq.edu.

**TABLE 1: Various Binding Energies (BEs) Utilizing Different Methods and Basis Sets<sup>a</sup>**

method	BE	BSSE	method	BE	BSSE
Haaland's estimation <sup>3</sup>	$\Delta H_{298} = -31.1 \pm 1.0$		MP2/aug-cc-pVDZ <sup>22</sup>	$\Delta E_0 = -23.5^b$	yes
Gurvich's estimation <sup>27</sup>	$\Delta H_{298} = -37.5 \pm 3.6$		CCSD(T)/aug-cc-pVTZ <sup>19</sup>	$\Delta E_{\text{elec}} = -31.1$	no
MP2/6-311++G(d,p) <sup>20</sup>	$\Delta E_0 = -26.5$	no	CCSD(T)/aug-cc-pVTZ <sup>19</sup>	$\Delta E_0 = -24.6$	no
B3LYP/6-311++G(d,p) <sup>20</sup>	$\Delta E_0 = -23.5$	no	B3LYP/6-31G(d) <sup>19</sup>	$\Delta E_{\text{elec}} = -32.8$	no
MPW1K/6-311++G(d,p) <sup>20</sup>	$\Delta E_0 = -28.1$	no	B3LYP/6-31G(d) <sup>19</sup>	$\Delta E_0 = -26.3$	no
CCSD(T)/6-311++G(d,p) <sup>21</sup>	$\Delta E_0 = -25.5$	no	G2(MP2) <sup>29</sup>	$\Delta E_0 = -26.0$	no
Piela's estimation <sup>22</sup>	$\Delta H_{298} = -25.7 \pm 2.0^b$	yes	MP2/6-31G(d,p) <sup>23</sup>	$\Delta H_{298} = -30.0$	no
CCSD(T)/aug-cc-pVDZ <sup>22</sup>	$\Delta E_{\text{elec}} = -28.5^b$	yes	MP2/6-31G(d,p) <sup>23</sup>	$\Delta H_{298} = -24.1$	yes
CCSD(T)/aug-cc-pVDZ <sup>22</sup>	$\Delta E_0 = -22.7^b$	yes	MP2/TZ2P <sup>24</sup>	$\Delta E_0 = -28.3$	no
CCSD(T)/aug-cc-pVDZ <sup>22</sup>	$\Delta H_{298} = -24.5^b$	yes	BLYP/6-31G(d) <sup>24</sup>	$\Delta E_0 = -28.5$	no
HF/aug-cc-pVDZ <sup>22</sup>	$\Delta E_{\text{elec}} = -20.1^b$	yes	CCSD(T)/cc-pVTZ <sup>24</sup>	$\Delta E_0 = -26.5$	no
HF/aug-cc-pVDZ <sup>22</sup>	$\Delta E_0 = -14.3^b$	yes	MP2/TZ2P <sup>17</sup>	$\Delta H_{298} = -30.7$	no
MP2/aug-cc-pVDZ <sup>22</sup>	$\Delta E_{\text{elec}} = -29.3^b$	yes	BAC-MP4 <sup>28</sup>	$\Delta H_{298} = -31.3$	no

<sup>a</sup> Binding enthalpies,  $\Delta H$ , electronic binding energies,  $\Delta E_{\text{elec}}$ , and ZPE corrected binding energies,  $\Delta E_0$ , are reported, indicating whether or not BSSE was corrected. All values are in kcal/mol. <sup>b</sup> The aug-cc-pVDZ basis set has been supplemented with diffuse f functions on the boron and nitrogen atoms and one diffuse d function on each hydrogen atom.

of ammonia borane is  $\Delta H_{298} = -31.1 \pm 1.0$  kcal/mol.<sup>3</sup> Second, Gurvich et al. used four experimental studies to estimate the heat of formation ( $-27.5 \pm 3.6$  kcal/mol) for  $\text{H}_3\text{B}-\text{NH}_3$ ,<sup>27</sup> which yields a B–N bond energy of 37.5 kcal/mol. It has been noted that Gurvich's estimated heats of formation were based upon experimental data not firmly established and that the large uncertainty could yield an inaccurate B–N binding enthalpy.<sup>28</sup>

Computational predictions of the  $\text{H}_3\text{B}-\text{NH}_3$  binding enthalpy are significantly weaker than the Haaland and Gurvich estimations. Predicted binding energies ( $\Delta E_0$ , corrected for zero-point energy (ZPE) at 0 K) are  $-24.6$  kcal/mol from CCSD(T)/aug-cc-pVTZ,<sup>19</sup>  $-26.5$  kcal/mol from MP2/6-311++G(d,p),<sup>20</sup> and  $-22.7$  from CCSD(T)/aug-cc-pVDZ.<sup>22</sup> Piela and co-worker's enthalpic estimation was determined by computing the binding enthalpy using MP2/aug-cc-pVDZ supplemented with a 3s3p2d1f set of functions centered in the middle of the B–N dative bond. The resulting binding enthalpy at 298 K was  $-26.5$  kcal/mol. The MP2 binding enthalpy was corrected by adding the correlation contribution of 0.8 kcal/mol, which is the difference between CCSD(T) and MP2 binding energies with the aug-cc-pVDZ basis set. The final estimated binding enthalpy reported at 298 K was  $-25.7 \pm 2.0$  kcal/mol.<sup>22</sup>

The B–N dative bond has been investigated computationally in substituted systems as well.<sup>18–21,23–25,29–32</sup> In particular, an investigation critiquing the ability of density functional theory to model B–N dative bonds accurately has been reported.<sup>20</sup> Systematic addition of methyl groups to the donor and acceptor atoms of ammonia borane revealed increasing error in B3LYP predicted binding energetics, whereas MP2 provided energetic trends consistent with experiment.<sup>20</sup> Other borate systems containing B–N dative bonds also have been analyzed in which B3LYP was unable to model the dative bond.<sup>21</sup> Further analysis showed that CCSD(T) predicted ZPE corrected binding energies<sup>21</sup> compare well with that predicted by MP2.<sup>20</sup>

The wide range of predicted binding energetics for  $\text{H}_3\text{B}-\text{NH}_3$  from  $-14.3$  to  $-37.5$  kcal/mol (Table 1) and the divergence of predicted binding energetics of substituted ammonia borane systems are symptomatic of the inherent difficulty in modeling the dative bond. The obvious variables contributing to the reported variability include the chemical method and basis set employed, whether BSSE corrections were implemented, and if the appropriate thermal corrections were applied to the electronic energy. Many of the reported studies recognize the need for one computational factor over another; however, in many of the reports, the energies were not corrected for BSSE, even though it is generally recognized that it ranges between 1 and 3 kcal/mol for density functional theory methods<sup>20</sup> and

between 3 and 10 kcal/mol for post-SCF methods.<sup>21–23,33</sup> BSSE corrections are important, because smaller basis sets are commonly used to predict the binding energetics of B–N dative bonds.

Due to the need for accurate computational modeling and characterization of the dative bond, a systematic computational approach has been implemented to investigate ammonia borane and methyl-substituted ammonia trimethylboranes ( $(\text{CH}_3)_3\text{B}-\text{N}(\text{CH}_3)_n\text{H}_{3-n}$ ;  $n = 0-3$ ). The  $(\text{CH}_3)_3\text{B}-\text{N}(\text{CH}_3)_n\text{H}_{3-n}$  complexes have been chosen for analysis rather than  $\text{H}_3\text{B}-\text{N}(\text{CH}_3)_n\text{H}_{3-n}$  systems, because more prominent effects on binding enthalpies have been observed.<sup>3</sup> The influence of electron correlation, basis set size, and BSSE have been considered by performing electronic structure calculations with a variety of basis sets, quantum chemical methods, and corrections to identify appropriate levels of theory that describe the dative bond. The relationship between the accurate prediction of charge-transfer frustration, ionicity, and covalency and the structural and energetic characterization of the dative bond has been evaluated to provide a more comprehensive understanding of the dative bond. Besides interest in the fundamental chemical physics of dative bonds,<sup>3,15</sup> this approach may be used as a predictive strategy for the structural and energetic properties of dative bonds that have important consequences in the fields of storage and release of hydrogen as a fuel,<sup>32,34,35</sup> growth of uniform coatings on individual filaments for fiber-reinforced ceramic matrix composites,<sup>36–40</sup> and as new oncological,<sup>41–43</sup> cardiovascular, and anti-inflammatory drugs.<sup>43,44,45–47</sup>

### Computational Details

All electronic structure calculations were carried out with the Gaussian 03 program<sup>48</sup> using the computational resources at the Center for Computational Sciences at Duquesne University. Full electronic structure optimizations (FOPT) on  $\text{H}_3\text{B}-\text{NH}_3$  were performed utilizing Hartree–Fock (HF), density functional theory (DFT), Møller–Plesset second-order perturbation theory (MP2),<sup>49,50</sup> and quadratic configuration interaction with single and double substitutions (QCISD)<sup>51</sup> in the gas phase. Single-point (SP) energy calculations have been employed utilizing QCISD incorporating a perturbational treatment of the triples contribution (QCISD(T))<sup>52</sup> on QCISD optimized geometries utilizing the same basis set as the QCISD optimization. Two DFT methods have been employed: the Becke three-parameter exchange functional<sup>53</sup> with the nonlocal correlation functional of Lee, Yang, and Parr (B3LYP)<sup>54</sup> and the modified Perdew–Wang one-parameter model for kinetics (MPW1K).<sup>55</sup> The

**TABLE 2: Number of Basis Functions Utilized by the Correlation-Consistent and Pople Style Basis Sets for H<sub>3</sub>B–NH<sub>3</sub><sup>a</sup>**

(X,Y)	Pople Basis Sets					
	6-31G(X,Y)	6-31+G(X,Y)	6-31++G(X,Y)	6-311G(X,Y)	6-311+G(X,Y)	6-311++G(X,Y)
(d)	42	50	56	54	62	68
(d,p)	60	68	74	72	80	86
(2d,p)	72	80	86	82	90	96
(2d,2p)	90	98	104	100	108	114
(3df,2p)	116	124	130	124	132	138
(3df,pd)	134	142	148	136	144	150
(3df,3pd)	170	178	184	172	180	186
(3d2f,3p2d)	220	228	234	216	224	230

X	Correlation-Consistent Basis Sets	
	cc-pVXZ	aug-cc-pVXZ
D	58	100
T	144	230
Q	290	436
5	512	734

<sup>a</sup> For correlation-consistent basis sets, X designates D, T, Q, or 5. For Pople style basis sets, X and Y designate polarization on all heavy atoms and hydrogen atoms, respectively.

methods have been combined with 48 Pople basis sets,<sup>56–62</sup> ranging from 6-31G(d) to 6-311++G(3d2f,3p2d) and from Dunning's cc-pVDZ to aug-cc-pV5Z correlation-consistent basis sets.<sup>63–66</sup> Due to resource issues, FOPTs could not be performed with QCISD or QCISD(T) with the aug-cc-pV5Z basis set. Consequently, SP energy calculations were performed with these levels of theory on MP2/6-311++G(3df,2p) optimized H<sub>3</sub>B–NH<sub>3</sub> geometries. A total of 336 levels of theory have been utilized, as shown in Table 2.

For the larger methyl-substituted ammonia boranes, (CH)<sub>3</sub>B–NH<sub>3</sub>, (CH)<sub>3</sub>B–NH<sub>2</sub>CH<sub>3</sub>, (CH)<sub>3</sub>B–NH(CH<sub>3</sub>)<sub>2</sub>, and (CH)<sub>3</sub>B–N(CH<sub>3</sub>)<sub>3</sub>, geometry optimizations with each of the methods up to MP2 coupled with the 6-311++G(3df,2p) basis set have been carried out. SP energy evaluations were conducted with QCISD and QCISD(T) with the 6-311++G(3df,2p) basis set on the geometry optimized MP2/6-311++G(3df,2p) structures. Also, the MP2 method has been employed with the 6-311++G(d,p) basis set to compare with previously reported ZPE corrected binding energies.<sup>20</sup>

All minima have been confirmed by the absence of imaginary frequencies by vibrational frequency calculations utilizing B3LYP/6-31G(d). Enthalpy corrections were predicted utilizing B3LYP/6-31G(d) and scaled by 0.9989<sup>67</sup> to predict binding enthalpies at 298 K for the H<sub>3</sub>B–NH<sub>3</sub> adduct. The scaling factor for computing enthalpies has been noted to be temperature-dependent.<sup>67</sup> Consequently, the scaling factor of 0.9941 has been interpolated (Figure S2 of the Supporting Information) from the data reported by Scott and Radom<sup>67</sup> to model the remaining four adducts, for which the experimental binding enthalpies have been determined at 373 K. The appropriately scaled enthalpy corrections were then added to the uncorrected electronic energy predicted at each of the 336 levels of theory to predict the binding enthalpies at 298 K for H<sub>3</sub>B–NH<sub>3</sub> and at 373 K for the trimethylboranes. When computing accurate binding energetics, it has been reported that BSSE should be corrected by utilizing the counterpoise method.<sup>22,68–73</sup> Thus, BSSE has been applied at all levels of theory by utilizing the counterpoise method developed by Boys and Bernardi.<sup>74</sup>

Natural bond orbital (NBO) analysis<sup>75</sup> was performed using the NBO 5.G program,<sup>76</sup> embedded within the Gaussian 03 program, to predict atomic charges derived from natural population analysis (NPA).<sup>77</sup> Atomic charges derived from NPA have been successful as effective measures of substituent-induced pK<sub>a</sub> shifts within a variety of anilines and phenols, able

to model the pK<sub>a</sub> shifts better than other charge partitioning schemes.<sup>78</sup> Furthermore, predicted NPA atomic charges were able to replicate electron density donating and withdrawing trends within substituted actinide complexes better than other methods of analysis.<sup>79</sup> Last, it was reported that the electronegativity equalization method should be based off atomic charges derived from the NPA scheme rather than those derived from other methods.<sup>80</sup>

All NBO computations have been performed with HF, B3LYP, MPW1K, and MP2 utilizing the 6-311++G(3df,2p) basis set on the corresponding optimized H<sub>3</sub>B–NH<sub>3</sub> and methyl-substituted ammonia trimethylborane structures. Natural resonance theory (NRT)<sup>75,81–83</sup> within NBO was employed to predict the bond order, bond covalencies, and bond ionicities corresponding to the B–N dative bond. NRT allows the determination of localized resonance structures and their corresponding weighting factors, expressing the contribution of each structure to the resonance hybrid. Subsequently, properties of a given delocalized system may be attained in resonance averaged form.

## Results and Discussion

**Convergence Rate and Value of B–N Dative Bond Length.** A systematic evaluation of H<sub>3</sub>B–NH<sub>3</sub> bond length across different chemical methods and basis sets has been carried out. The rate of bond length convergence as a function of the number of basis functions and the converged value have been compared to the reported experimental B–N bond length of 1.658 ± 0.002 Å, determined by microwave spectra of nine isotopic species of ammonia borane between 308 and 318 K.<sup>84</sup> A prior microwave spectra analysis of two isotopic species determined that the B–N bond length was 1.66 ± 0.03 Å,<sup>85</sup> where assumptions made resulted in a larger standard deviation. The more recent account performed a full isotopic substitution, allowing the assumed parameters to be determined directly, allowing a more accurate B–N bond length to be reported.

Recent computational work has been shown to reach accuracies of ±0.001 Å in bond lengths.<sup>86</sup> High accuracy also has been achieved by Feller and Peterson by employing high-level calculations on 68 molecules, including elements from the first four rows of the periodic table.<sup>87</sup> However, such accurate results are only achieved with a minimum CCSD(T)/aug-cc-pV5Z quality level of theory, including a complete basis set extrapolation, core/valence and scalar relativistic effects, additional

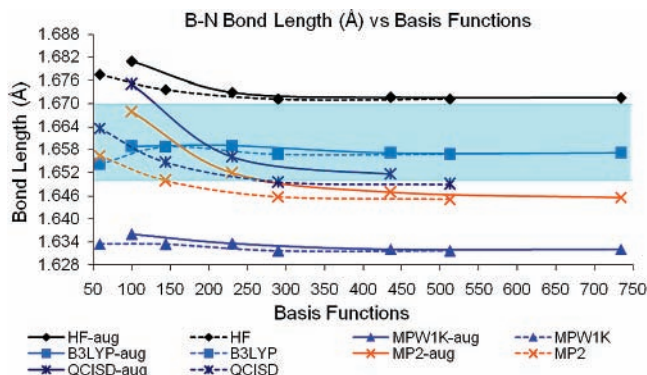


**Figure 1.** Convergence behavior of the B–N dative bond length (Å) vs number of basis functions for HF, B3LYP, MPW1K, MP2, and QCISD employed with aug-cc-pVXZ (solid line) and cc-pVXZ (dashed line), where X is D, T, Q, or 5. The correspondence between the number of basis functions and the basis set is given in Table 2. The light blue area represents the range of uncertainty for the experimental gas-phase result of  $1.66 \pm 0.01$ .<sup>84</sup>

corrections accounting for higher order correlation via CCSDTQ, and second-order spin–orbit effects. These specific calculations are resource intensive and limited to small systems, such as  $C_2$  and  $O_2H$ .<sup>87</sup> However, accuracies of  $\pm 0.01$  Å have been acquired with CCSD(T)/aug-cc-pVQZ on the G2 collection of molecules.<sup>88</sup> Since the present investigation employs a similar quality level of theory, a reasonable and expected uncertainty in the predicted B–N length is 0.01 Å. Consequently, all computations in this study have been compared to a B–N bond length of  $1.66 \pm 0.01$  Å, despite the experimental uncertainty of  $\pm 0.002$  Å.

The correlation-consistent basis sets,<sup>63–66</sup> ranging from cc-pVDZ to aug-cc-pV5Z, have been used for the geometry optimization of  $H_3B-NH_3$ , due to the systematic inclusion of electron correlation and possible extrapolation to the complete basis set limit.<sup>89–91</sup> Convergence was estimated when the change in bond length between consecutive basis sets was less than  $1 \times 10^{-3}$  Å and for all subsequent pairwise comparisons. For each chemical method utilized, smooth convergence is observed with and without augmentation, as shown in Figure 1.

A number of important issues arise when considering how the bond length depends upon the number and type of basis functions utilized in the basis set. First, the inclusion of diffuse functions lengthens post-SCF bond lengths for smaller basis sets. For example, bond lengths modeled from correlation consistent basis sets with augmentation converge between aug-cc-pVQZ (436 basis functions) and aug-cc-pV5Z (734 basis functions) for HF and each DFT method, where the cc-pVXZ basis sets (no augmentation) converge by 290 basis functions. Second, DFT and HF need less than half the basis functions to achieve convergence as compared to post-SCF methods, when augmentation is considered. Third, Hartree–Fock overestimates the experimental bond length by 0.012 Å, whereas B3LYP, QCISD, MP2, and MPW1K underestimate experiment by 0.003, 0.011, 0.014, and 0.028 Å, respectively. Thus, all methods using correlation-consistent basis sets converge within 1% of the reported experimental value, except MPW1K. The B–N length predicted by B3LYP is the only method that converges within the accuracy of 0.01 Å using the correlation-consistent basis sets. However, bond lengths predicted by HF, QCISD, and MP2 converge outside the experimental uncertainty of  $\pm 0.002$  Å by 0.002, 0.0010, and 0.004 Å, respectively. Importantly, post-SCF methods converge to shorter B–N bond lengths than those predicted by experiment. This behavior is anticipated because

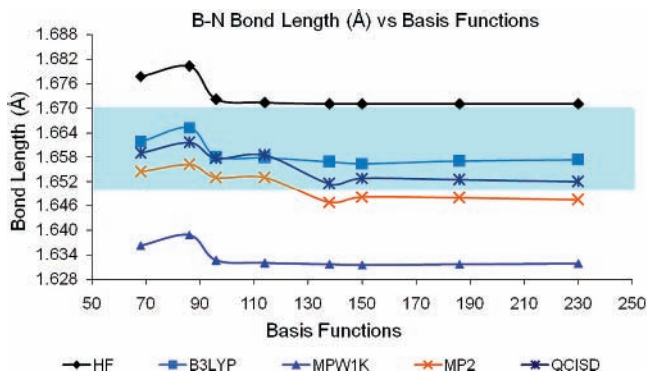


**Figure 2.** Convergence behavior of the B–N dative bond length (Å) vs number of basis functions for HF, B3LYP, MPW1K, MP2, and QCISD employed with the 6-311++G(X,Y) basis sets where X and Y represent additional polarization functions. The correspondence between the number of basis functions and the basis set is given in Table 2. The light blue area represents the range of uncertainty for the experimental gas-phase result of  $1.66 \pm 0.01$ .<sup>84</sup>

the predicted geometries are computed at 0 K, whereas the experimental values were determined between 308 and 318 K.

Figure 2 displays the B–N dative bond lengths modeled using Pople style 6-311++G(X,Y) basis sets with different chemical methods. Predicted lengths by post-SCF methods converge to a B–N bond length near 150 basis functions (6-311++G(3df,-pd)), whereas DFT and HF converge earlier at 96 basis functions (6-311++G(2d,p)). The converged bond lengths for all methods range between 1.63 and 1.67 Å, which is in good agreement with experiment.<sup>84</sup> The same order in increasing bond length with Pople basis sets is observed as with the correlation-consistent basis sets (HF > B3LYP > QCISD > MP2 > MPW1K). Only B3LYP and QCISD with the 6-311++G(X,Y) basis sets converge within the accuracy of 0.01 Å. HF and MP2 converge within 0.001 Å of the upper bound error ( $1.658 + 0.002$  Å) and 0.003 Å of the lower bound error ( $1.658 - 0.002$  Å), respectively. All B–N bond lengths employing the 6-311++G(X,Y) basis sets converged to the bond lengths predicted by the correlation-consistent basis sets within 0.2%.

The predicted bond lengths (converged and not converged) by all chemical methods and basis sets utilized in this study (Figure S3 and Table S1 of the Supporting Information) range between 1.63 and 1.69 Å, again in good agreement with experiment.<sup>84</sup> There are a few notable points. For example, double- $\zeta$  split-valence quality basis sets (i.e., 6-31G(X,Y), 6-31+G(X,Y), and 6-31++G(X,Y)) do not necessarily produce a converged B–N bond length. In fact, the predicted change in bond length by DFT methods and HF never converged. Post-SCF methods also had trouble yielding a converged B–N bond length for the double- $\zeta$  basis sets but converged when employing 3df and 3dp polarization functions on the heavy and hydrogen atoms, respectively.

In general, the quality of the basis set is important to predicting the B–N bond length. The triple- $\zeta$  split-valence quality basis sets (i.e., 6-311G(X,Y), 6-311+G(X,Y), and 6-311++G(X,Y)) yielded converged B–N bond lengths. In particular, the 6-311++G(X,Y) basis sets converged smoothly to the bond length yielded by the correlation-consistent basis sets and were found to be within or near the accuracy of  $\pm 0.01$  Å for most methods employed. In the final assessment, the 6-311++G(3df,pd) and 6-311++G(2d,p) basis sets (150 and 96 basis functions, respectively) or greater are necessary to ensure a converged B–N dative bond length for post-SCF methods and DFT or HF methods, respectively.

**TABLE 3: BSSE Uncorrected Binding Enthalpies,  $\Delta H_{298}$  (kcal/mol), Predicted Utilizing Structures from SP and FOPT Calculations<sup>a</sup>**

	$\Delta H_{298}$ SP	$\Delta H_{298}$ FOPT higher level	B–N FOPT higher level	B–N FOPT lower level	$\Delta B-N$	$\Delta\Delta H_{298}$
Longest B–N bond length						
MP2/aug-cc-pVDZ//HF/6-31G(d)	–26.7	–26.6	1.668	1.689	0.021	0.1
MP2/aug-cc-pVTZ//HF/6-31G(d)	–27.6	–27.8	1.652	1.689	0.037	0.2
MP2/aug-cc-pVQZ//HF/6-31G(d)	–27.9	–28.1	1.647	1.689	0.042	0.2
Shortest B–N bond length						
MP2/aug-cc-pVDZ//MPW1K/6-31G(2d,2p)	–26.5	–26.6	1.668	1.632	0.036	0.1
MP2/aug-cc-pVTZ//MPW1K/6-31G(2d,2p)	–27.8	–27.8	1.652	1.632	0.020	0.0
MP2/aug-cc-pVQZ//MPW1K/6-31G(2d,2p)	–28.1	–28.1	1.647	1.632	0.015	0.0
Justification of QCISD SP						
QCISD/aug-cc-pVDZ//MP2/6-311++G(3df,2p)	–24.7	–24.6	1.675	1.647	0.028	0.1
QCISD/6-311++G(d,p)//MP2/6-311++G(3df,2p)	–26.1	–26.1	1.662	1.647	0.015	0.0
QCISD/6-311++G(3df,2p)//MP2/6-311++G(3df,2p)	–26.2	–26.2	1.652	1.647	0.005	0.0
<hr/>						
	$\Delta H_{298}$					$\Delta H_{298}$
Justification of QCISD(T) SP						
QCISD(T)/aug-cc-pVDZ//QCISD/aug-cc-pVDZ	–25.7	QCISD(T)/aug-cc-pVDZ//MP2/6-311++G(3df,2p)				–25.7
QCISD(T)/6-311++G(d,p)//QCISD/6-311++G(d,p)	–27.4	QCISD(T)/6-311++G(d,p)//MP2/6-311++G(3df,2p)				–27.4
QCISD(T)/6-311++G(3df,2p)//QCISD/6-311++G(3df,2p)	–27.4	QCISD(T)/6-311++G(3df,2p)//MP2/6-311++G(3df,2p)				–27.5

<sup>a</sup> Bond lengths and differences are reported in angstroms. Differences in binding enthalpies ( $\Delta\Delta H_{298}$ ) are reported in kcal/mol.

**Sensitivity of Binding Enthalpy upon B–N Dative Bond Length.** To investigate the energetic sensitivity upon bond length variation, binding enthalpies determined by MP2/aug-cc-pVXZ (X = D, T, and Q) SP energy calculations employed on the shortest and longest B–N bond lengths across all levels of theory considered were compared to binding enthalpies resulting from full geometry optimizations at the MP2/aug-cc-pVXZ level of theory. MP2 has been chosen due to its accuracy and efficiency, as discussed later. The longest B–N bond length of 1.689 Å resulted from HF/6-31G(d), and the shortest of 1.632 Å was located using MPW1K/6-31G(2d,2p). Table 3 displays the predicted binding enthalpies, B–N dative bond lengths, and corresponding differences between the higher and the lower levels of theory. The largest binding enthalpy difference predicted was 0.2 kcal/mol. Thus, the data indicate that the predicted B–N bond length variation using different levels of theory does not account for the wide discrepancy of binding energies reported in Table 1.

Considering post-SCF methods, the B–N bond length converges at the 6-311++G(3df,pd) basis set. However, binding enthalpies converge earlier, as discussed later, at the similar 6-311++G(3df,2p) basis set. The use of 6-311++G(3df,2p) over 6-311++G(3df,pd) saves 12 basis functions for H<sub>3</sub>B–NH<sub>3</sub> and 36 for the largest methyl-substituted ammonia trimethylborane considered. Despite the resource savings, FOPTs remain impractical on the larger methyl-substituted ammonia trimethylborane structures with available resources utilizing QCISD and QCISD(T) with either basis set. However, SP energy evaluations were possible with QCISD and QCISD(T) using the 6-311++G(3df,2p) basis set with BSSE corrections. To justify this approach, QCISD SP energy evaluations using small (aug-cc-pVDZ) to large (6-311++G(3df,2p)) basis sets on MP2/6-311++G(3df,2p) optimized H<sub>3</sub>B–NH<sub>3</sub> structures were compared to QCISD/6-311++G(3df,2p) FOPT energies. As shown in Table 3, there is negligible (<0.1 kcal/mol) difference between binding enthalpy determined by the QCISD FOPTs and SPs. Finally, SP energies using QCISD(T) with different basis sets on QCISD and MP2 optimized structures were compared. As seen in Table 3, QCISD(T)//QCISD binding enthalpies differ from QCISD(T)//MP2 values by an insignificant amount (<0.1 kcal/mol). The data suggest that performing

QCISD and QCISD(T) SP computations on MP2 optimized structures is a valid approximation to analyze the larger trimethylboranes. Consequently, energy evaluations were conducted employing the 6-311++G(3df,2p) basis set rather than 6-311++G(3df,pd).

**Impact of BSSE upon Binding Enthalpy for H<sub>3</sub>B–NH<sub>3</sub>.** The influence of BSSE has been well-documented<sup>21–23,33,69–73</sup> but has been inconsistently applied in reports on the dative bond, as summarized in Table 1. To investigate the impact of this factor on dative bonding systematically, BSSE has been determined for each method utilizing the correlation-consistent basis sets, as shown in Figure 3. In general, the BSSE corrected binding enthalpies are weaker than those not corrected for BSSE.

Two interesting trends on the BSSE corrected binding enthalpies are observed. First, cc-pVXZ basis sets result in more BSSE than the augmented basis sets, especially with smaller basis sets. Second, post-SCF computations result with increased BSSE, as compared to DFT and HF. It has been noted previously that methods incorporating electron correlation result in more BSSE as compared to HF and DFT methods with smaller basis sets.<sup>21,23,33,73</sup> For example with the cc-pVDZ basis set (58 basis functions), post-SCF methods, DFT, and HF methods incorporate BSSE on the order of ca. 7.0, 4.5, and 3.5 kcal/mol, respectively. BSSE is practically eliminated (0.0–0.4 kcal/mol) with the use of the cc-pV5Z basis set (512 basis functions). More specifically, BSSE is completely removed for DFT and HF with the use of the aug-cc-pVTZ basis set (230 basis functions), whereas aug-cc-pVQZ (436 basis functions) is needed to eliminate BSSE (0.2–0.4 kcal/mol) for post-SCF methods. The same trend is seen for the Pople basis sets, where basis sets lacking diffuse functions incorporate more BSSE than those that include diffuseness. BSSEs for all basis sets and methods and the BSSE uncorrected binding enthalpies are reported in Tables S4 and S2 of the Supporting Information, respectively. In general, the basis sets typically employed (Table 1) in the evaluation of the dative bond are too small and require the adjustment for BSSE. However, these smaller basis sets result in energetics far from convergence.

**Convergence of Binding Enthalpy for H<sub>3</sub>B–NH<sub>3</sub> with BSSE Corrections.** The binding enthalpy convergence for H<sub>3</sub>B–NH<sub>3</sub> was analyzed in the same manner as the bond length.

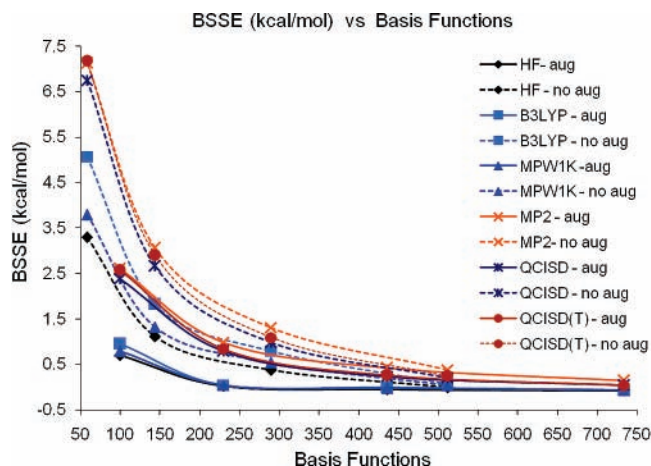


**Figure 3.** BSSE (kcal/mol) for HF, B3LYP, MPW1K, MP2, QCISD, and QCISD(T) utilizing the cc-pVXZ (dashed lines) and aug-cc-pVXZ (solid lines) basis sets. The BSSE is determined by subtracting the uncorrected  $\Delta H_{298}$  from the BSSE corrected  $\Delta H_{298}$ . QCISD and QCISD(T) corrections employed with the aug-cc-pv5z basis set are performed on the MP2/6-311++G(3df,2p) optimized structure.

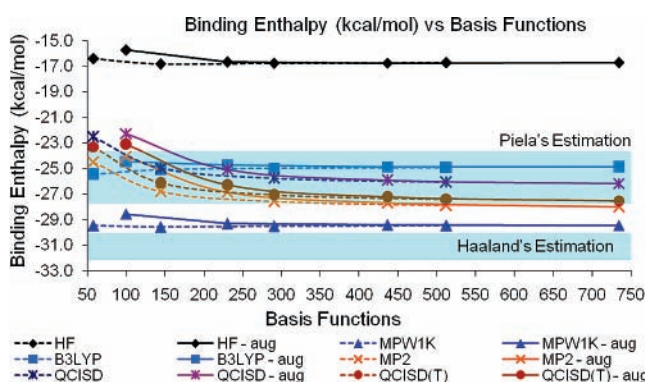


**Figure 4.** Predicted binding enthalpies,  $\Delta H_{298}$  (kcal/mol), for  $H_3B-NH_3$  versus basis functions with aug-cc-pVXZ and cc-pVXZ (X = D, T, Q, and 5) correlation-consistent basis sets for HF, B3LYP, MPW1K, MP2, QCISD, and QCISD(T) with BSSE corrections. The light blue areas represent Piela's and Haaland's estimations of  $-31.1 \pm 1.0$  and  $-25.7 \pm 2.0$  kcal/mol, respectively. The Gurvich estimation is not shown on the figure. The QCISD(T)/aug-cc-pV5Z data point is a SP energy evaluation on the MP2/6-311++G(3df,2p) optimized structure.

The rate of binding enthalpy convergence with BSSE corrections as a function of the number of basis functions has been determined, and the converged value has been compared to estimations provided by Haaland ( $-31.1 \pm 1.0$  kcal/mol),<sup>3</sup> Gurvich ( $-37.5 \pm 3.6$  kcal/mol),<sup>27</sup> and Piela ( $-25.7 \pm 2.0$  kcal/mol).<sup>22</sup> The experimental binding enthalpy has not been reported. Convergence was identified when the change in binding enthalpy between consecutive basis sets, and for all subsequent pairwise comparisons, was less than 0.3 kcal/mol. For each chemical method utilized, smooth convergence is observed for the correlation-consistent basis sets with and without augmentation, as shown by Figure 4.

Three important conclusions can be drawn concerning the predicted BSSE corrected  $\Delta H_{298}$ . First, the inclusion of diffuse functions is significant for smaller basis set computations, such as those reported in Table 1. Each method with augmentation underestimates the converged binding enthalpy by several kcal/mol up until ca. 225 basis functions. Second, the binding enthalpy convergence is slower using post-SCF methods as compared to DFT and HF. For example, MP2, QCISD, and QCISD(T) binding enthalpies continue to change by 0.2–0.3 kcal/mol between cc-pVQZ and cc-pV5Z with and without augmentation. Further evaluation using cc-pV6Z is currently not possible due to resource limitations. In contrast, DFT and

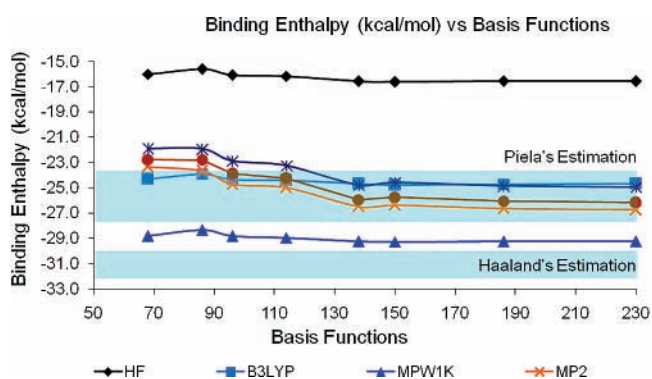


**Figure 5.** Predicted binding enthalpies,  $\Delta H_{298}$  (kcal/mol), for  $H_3B-NH_3$  versus number of basis functions with 6-311++G(X,Y) for HF, B3LYP, MPW1K, MP2, QCISD, and QCISD(T) with BSSE corrections. The light blue areas represent Piela's and Haaland's estimations of  $-31.1 \pm 1.0$  and  $-25.7 \pm 2.0$  kcal/mol, respectively. The Gurvich estimation is not shown on the figure.

HF converge earlier between cc-pVTZ (144 basis functions) and aug-cc-pVTZ (230 basis functions). Third, the DFT and post-SCF binding enthalpy predictions fall between the Piela and Haaland estimates. As expected, the order of converged binding enthalpies supports the order of B–N bond lengths. The weakest to strongest binding enthalpies are HF < B3LYP < QCISD < QCISD(T) < MP2 < MPW1K. Both HF and MPW1K are in poor energetic agreement with the previous estimates. Last, the BSSE corrected  $\Delta H_{298}$  converges to the same BSSE uncorrected  $\Delta H_{298}$  for each method.

For Pople basis sets, the convergence of the BSSE corrected  $\Delta H_{298}$  has been analyzed using the 6-311++G(X,Y) basis sets, which is shown by Figure 5. All methods utilizing the 6-311++G(3df,2p) basis set converged to the binding enthalpies predicted by correlation-consistent basis sets (cc-pVTZ and aug-cc-pVTZ for DFT and HF), except post-SCF methods. MP2, QCISD, and QCISD(T) with the 6-311++G(3df,2p) basis set predict a weaker binding enthalpy than with the aug-cc-pV5Z basis set by 1.5, 1.3, and 1.6 kcal/mol, respectively. It is found that the post-SCF predicted BSSE corrected binding enthalpies converge slowly and do not converge even when the large Pople basis set is employed. It is assumed that the BSSE corrected  $\Delta H_{298}$  prediction with post-SCF methods utilizing the 6-311++G(X,Y) basis sets will converge eventually to that predicted by the aug-cc-pV5Z basis set, with increased polarization functions, as found for the B–N bond lengths. As a consequence, the

**TABLE 4: BSSE Corrected and Experimental Binding Enthalpies (kcal/mol) at 373 K,  $\Delta H_{373}$ , for  $(\text{CH}_3)_3\text{B}-\text{N}(\text{CH}_3)_n\text{H}_{3-n}$ ;  $n = 0-3^a$** 

	$\text{B}(\text{CH}_3)_3-\text{NH}_3$	$\text{B}(\text{CH}_3)_3-\text{NH}_2\text{CH}_3$	$\text{B}(\text{CH}_3)_3-\text{NH}(\text{CH}_3)_2$	$\text{B}(\text{CH}_3)_3-\text{N}(\text{CH}_3)_3$	MAD
MPW1K/6-311++G(3df,2p)	-11.9	-14.2	-12.9	-9.1	5.1
B3LYP/6-311++G(3df,2p)	-6.8	-8.8	-7.0	-2.4	10.8
HF/6-311++G(3df,2p)	-2.0	-3.5	-1.2	3.6	16.3
MP2/6-311++G(d,p) <sup>b</sup>	-15.4	-20.4	-22.1	-21.4	2.8
MP2/6-311++G(d,p)	-11.0	-15.1	-15.9	-14.3	3.0
MP2/6-311++G(3df,2p)	-15.6 (-14.1)	-20.1 (-18.6)	-21.4 (-19.9)	-20.2 (-18.7)	2.2 (0.7)
QCISD/6-311++G(3df,2p)	-12.6 (-11.3)	-13.8 (-12.5)	-16.8 (-15.5)	-14.7 (-13.4)	2.6 (3.9)
QCISD(T)/6-311++G(3df,2p)	-14.4 (-12.8)	-18.6 (-17.0)	-19.5 (-17.9)	-17.8 (-16.2)	0.5 (1.1)
experiment <sup>26</sup>	-13.8 $\pm$ 0.3	-17.6 $\pm$ 0.2	-19.3 $\pm$ 0.3	-17.6 $\pm$ 0.2	

<sup>a</sup> Values within parentheses do not account for convergence corrections of 1.5, 1.3, and 1.6 kcal/mol for MP2, QCISD, and QCISD(T), respectively. Mean absolute deviations (MADs) from experimental data are reported. <sup>b</sup> From ref 19, which are not corrected for BSSE nor thermal corrections. Only ZPE corrections are applied.

**TABLE 5: Factors Influencing the QCISD(T) Predicted Binding Energetics (kcal/mol), for  $\text{H}_3\text{B}-\text{NH}_3$  and  $(\text{CH}_3)_3\text{B}-\text{N}(\text{CH}_3)_n\text{H}_{3-n}$ ;  $n = 0-3^a$** 

	average difference (kcal/mol)	$\text{H}_3\text{B}-\text{NH}_3$ $T = 298 \text{ K}$	$\text{B}(\text{CH}_3)_3-\text{NH}_3$ $T = 373 \text{ K}$	$\text{B}(\text{CH}_3)_3-\text{NH}_2\text{CH}_3$ $T = 373 \text{ K}$	$\text{B}(\text{CH}_3)_3-\text{NH}(\text{CH}_3)_2$ $T = 373 \text{ K}$	$\text{B}(\text{CH}_3)_3-\text{N}(\text{CH}_3)_3$ $T = 373 \text{ K}$
$\Delta E_{\text{elec}}$	0.0	-31.5 (0.0)	-18.1 (0.0)	-22.6 (0.0)	-24.1 (0.0)	-23.1 (0.0)
$\Delta E_{\text{elec}} + \text{BSSE corrections}$	2.7	-29.9 (1.7)	-15.7 (2.4)	-19.9 (2.7)	-21.0 (3.1)	-19.5 (3.6)
$\Delta E_0 + \text{BSSE corrections}$	7.2	-24.3 (7.3)	-11.2 (6.9)	-15.9 (6.7)	-17.0 (7.1)	-15.2 (7.9)
$\Delta H_T + \text{BSSE corrections}$	5.9	-25.9 (5.6)	-12.8 (5.3)	-17.0 (5.6)	-17.9 (6.2)	-16.2 (6.9)

<sup>a</sup> Relative values to the predicted binding electronic energy,  $\Delta E_{\text{elec}}$ , are given in parentheses. The convergence correction of 1.6 kcal/mol for QCISD(T) is not applied.

residual errors of 1.5, 1.3, and 1.6 kcal/mol for MP2, QCISD, and QCISD(T), respectively, called the “convergence correction”, will be subtracted (increase the magnitude) from the predicted  $\Delta H_{373}$  for methyl-substituted ammonia trimethylboranes discussed in the next section. Other basis sets are reported in Figure S4 and Table S3 of the Supporting Information.

Our final prediction for the binding enthalpy at 298 K is  $-27.5 \pm 0.5$  kcal/mol, using QCISD(T)/aug-cc-pV5Z on the MP2/6-311++G(3df,2p) optimized geometry. BSSE is negligible when the aug-cc-pV5Z basis set is employed. The error of 0.5 kcal/mol is estimated from the QCISD(T) mean absolute deviation (MAD) of four methyl-substituted ammonia trimethylboranes analyzed and discussed in the next section. The error of 0.5 kcal/mol is not unreasonable, because high accuracy compound methods, such as Gaussian-4, report energetics with an average absolute deviation of 0.80 kcal/mol.<sup>92</sup> Our prediction is within the uncertainty of Piela’s  $-25.7 \pm 2.0$  kcal/mol,<sup>22</sup> yet significantly weaker than Haaland’s estimate of  $-31.1 \pm 1.0$  kcal/mol<sup>3</sup> and Gurvich’s recommendation of  $-37.5 \pm 3.6$  kcal/mol.<sup>27</sup>

**Analysis of  $\Delta H_{373}$  for  $(\text{CH}_3)_3\text{B}-\text{N}(\text{CH}_3)_n\text{H}_{3-n}$ ;  $n = 0-3$ .** The binding enthalpies of the four methyl-substituted ammonia trimethylboranes,  $(\text{CH}_3)_3\text{B}-\text{NH}_3$ ,  $(\text{CH}_3)_3\text{B}-\text{NH}_2\text{CH}_3$ ,  $(\text{CH}_3)_3\text{B}-\text{NH}(\text{CH}_3)_2$ , and  $(\text{CH}_3)_3\text{B}-\text{N}(\text{CH}_3)_3$ , have been predicted with each method using the 6-311++G(3df,2p) basis set with BSSE and convergence corrections and compared with experiment.<sup>26</sup> Table 4 displays the BSSE corrected binding enthalpies at 373 K with and without the convergence correction for the post-SCF methods.

Ammonia borane has the strongest dative bond, as compared to any of the methyl-substituted systems. However, beyond  $(\text{CH}_3)_3\text{B}-\text{NH}_2\text{CH}_3$ , experiment gives an increase in B–N dative bond strength for each methyl group added to the nitrogen atom, until the third methyl group, in which the B–N dative bond strength decreases to that of the one methyl case. Although DFT and HF are less affected by BSSE, these methods are unable to model the experimental  $\Delta H_{373}$  values and trends accurately. All DFT and HF methods predict that the addition of the second

methyl group will decrease the B–N dative bond strength, which contradicts the experimental trend. HF, B3LYP, and MPW1K are also unable to model the B–N binding enthalpy on a quantitative level as well, evident by MADs of 16.3, 10.8, and 5.1 kcal/mol (Table 4), respectively.

All post-SCF methods with the 6-311++G(3df,2p) basis set incorporating BSSE and convergence corrections reproduced the experimental trend of increasing then decreasing B–N dative bond strength with MADs of 2.2, 2.6, and 0.5 kcal/mol for MP2, QCISD, and QCISD(T), respectively. The BSSE and convergence corrected QCISD(T) binding enthalpies are within the experimental uncertainty for trimethylboranes ( $n = 2$  and 3) and slightly outside the experimental accuracy by 0.3 and 0.8 kcal/mol for  $n = 0$  and 1, respectively. The data suggest that the triples correction of the wave function is critical, accounting for ca. 10–25% of the  $\Delta H_{373}$  to align computation with experiment.

**Significance of Thermal Corrections.** The ability of theory to predict accurate B–N dative binding enthalpies has been shown to depend upon the method, basis set size and functions, and BSSE. However, thermal corrections can also make important contributions to the predicted binding energetics. For example, the thermal adjustments with BSSE associated with the highest level of theory employed, QCISD(T)/6-311++G(3df,2p)/MP2/6-311++G(3df,2p), are listed in Table 5.

As expected, thermal factors are found to influence the predicted binding energetics significantly, yet are not always applied for comparison with experiment. BSSE alone can account for an absolute difference from the binding electronic energy by up to 3.6 kcal/mol, BSSE and zero-point energy corrections up to 7.9 kcal/mol, and BSSE and enthalpic (thermal) corrections up to 6.9 kcal/mol. This does not mean that the predicted binding energetics are necessarily incorrect; however, care must be taken for valid comparison with experiment. For example, the predicted  $\Delta E_{\text{elec}}$  for  $\text{H}_3\text{B}-\text{NH}_3$  is  $-31.5$  kcal/mol using QCISD(T)/6-311++G(3df,2p), which is in fortuitous agreement with Haaland’s estimation of  $-31.1 \pm 1.0$  kcal/mol. Haaland’s estimation is not a  $\Delta E_{\text{elec}}$  value rather an extrapolation

**TABLE 6: Factors Influencing the MP2/6-311++G(d,p) Predicted Binding Energetics (kcal/mol) for H<sub>3</sub>B–NH<sub>3</sub> and (CH<sub>3</sub>)<sub>3</sub>B–N(CH<sub>3</sub>)<sub>n</sub>H<sub>3–n</sub>; n = 0–3<sup>a</sup>**

	average difference (kcal/mol)	H <sub>3</sub> B–NH <sub>3</sub> T = 298 K	B(CH <sub>3</sub> ) <sub>3</sub> –NH <sub>3</sub> T = 373 K	B(CH <sub>3</sub> ) <sub>3</sub> –NH <sub>2</sub> CH <sub>3</sub> T = 373 K	B(CH <sub>3</sub> ) <sub>3</sub> –NH(CH <sub>3</sub> ) <sub>2</sub> T = 373 K	B(CH <sub>3</sub> ) <sub>3</sub> –N(CH <sub>3</sub> ) <sub>3</sub> T = 373 K
$\Delta E_{\text{elec}}$	0.0	–32.0 (0.0)	–19.9 (0.0)	–24.4 (0.0)	–26.1 (0.0)	–25.7 (0.0)
$\Delta E_{\text{elec}} + \text{BSSE corrections}$	6.4	–27.6 (4.3)	–13.9 (6.0)	–18.0 (6.4)	–19.0 (7.1)	–17.5 (8.2)
$\Delta E_0 + \text{BSSE corrections}$	11.0	–21.1 (10.8)	–9.4 (10.5)	–14.0 (10.4)	–14.9 (11.1)	–13.3 (12.4)
$\Delta H_T + \text{BSSE corrections}$	9.6	–23.7 (8.3)	–11.0 (8.9)	–15.1 (9.3)	–15.9 (10.2)	–14.3 (11.4)

<sup>a</sup> Relative values to the predicted electronic binding energy,  $\Delta E_{\text{elec}}$ , are given in parentheses.

from  $\Delta H_{298}$  values. When the appropriate thermal corrections are applied to the QCISD(T) prediction,  $\Delta H_{298}$  is predicted to be –25.9 kcal/mol, which is 5.2 kcal/mol different from Haaland's. Thus, without a systematic study, it is possible for theory and experimental values to match accidentally; however, this could be avoided when proper corrections are applied. Consequently, with larger thermal factors, the methyl-substituted ammonia trimethylboranes require thermal adjustments for accurate experimental comparison.

When a lower level of theory is utilized, such as with MP2/6-311++G(d,p), the corrections are larger (Table 6) due to BSSE. Since each level of theory is corrected by the same scaled frequencies (see Computational Details section), BSSE is the only variable in this study. However, the binding electronic energy can change up to 8.2 kcal/mol, BSSE and ZPE corrections up to 12.4 kcal/mol, and BSSE and enthalpic (thermal) corrections up to 11.4 kcal/mol. The results demonstrate the importance of thermal corrections and BSSE.

It has been previously recommended that the MP2 method employed with at least a triple- $\zeta$  split-valence basis set should be utilized to model the B–N dative bond.<sup>20,21</sup> Evaluation of the methyl-substituted ammonia trimethylboranes utilizing MP2/6-311++G(d,p) reveals that BSSE ranges between 6.0 and 8.2 kcal/mol, as shown in Table 6. The comparison with experiment should include thermal and BSSE corrections. For example, the MP2/6-311++G(d,p) BSSE uncorrected binding energies employing only ZPE corrections for (CH<sub>3</sub>)<sub>3</sub>B–N(CH<sub>3</sub>)<sub>n</sub>H<sub>3–n</sub>, where *n* is 0, 1, 2, and 3, are –15.4, –20.4, –22.1, and –21.4 kcal/mol (MAD of 2.8 kcal/mol),<sup>20</sup> respectively. The reported values and differences are significantly different than the MP2/6-311++G(d,p) predicted binding enthalpies of –11.0, –15.1, –15.9, and –14.3 kcal/mol (MAD of 3.0 kcal/mol), respectively, which are adjusted for thermal factors (373 K) and BSSE.

There are three key conclusions. First, the electronic energy should be adjusted with the necessary thermodynamic corrections at the appropriate temperature for a proper comparison with experiment. Second, the 6-311++G(3df,2p) basis set should be utilized with the convergence correction of 1.3–1.6 kcal/mol to ensure a converged and accurate binding enthalpy. Last, BSSE must be implemented to predict the binding enthalpy accurately. It is recommended that if accurate binding enthalpies are desired on a quantitative level (MAD of 0.5 kcal/mol), then single-point energy calculations utilizing QCISD(T)/6-311++G(3df,2p) should be utilized, incorporating BSSE corrections as well as the 1.6 kcal/mol convergence correction on MP2/6-311++G(3df,2p) optimized structures. However, if semiquantitative results are desired (MAD of 2.2 kcal/mol), maintaining the qualitative trend, then the full optimizations utilizing MP2/6-311++G(3df,2p) should be employed, incorporating BSSE corrections as well as the 1.5 kcal/mol convergence correction. MP2 utilized with the 6-311++G(3df,2p) basis set offers an appropriate balance of accuracy and efficiency to model the energetics of B–N dative bonds. These two levels of theory

may be utilized to model the structural and energetic properties of B–N dative bonds.

**Chemical Descriptors of the B–N Dative Bond.** To probe the electronic nature of the dative bond, NBO and NRT analysis has been employed to provide the chemical descriptors (atomic charges, bond orders, bond covalency, bond ionicity, and charge-transfer frustration) within H<sub>3</sub>B–NH<sub>3</sub> and the four methyl-substituted ammonia trimethylboranes. QCISD(T)/6-311++G(3df,2p) with BSSE and convergence corrections has been shown to predict accurate binding enthalpies for substituted trimethyl boranes. However, the electronic wave function predicted by QCISD(T) cannot be analyzed by NBO, because the requisite density matrix is not available. Thus, due to its proven semiquantitative results, MP2/6-311++G(3df,2p) predicted charges, bond orders, covalencies, and ionicities, and binding enthalpies with BSSE and convergence corrections are taken as the reference for further calculations. To uncover the “physical” reasons for the wide variability in predicted binding enthalpies by different levels of theory, NBO and NRT analysis has been performed with HF, B3LYP, and MPW1K utilizing the 6-311++G(3df,2p) basis set on the corresponding optimized structures and compared back to the MP2 results for percent error calculations. Thus, MP2 is the reference point or considered to be “exact” for the percent error calculations and will be included in the data sets.

**Charge-Transfer Frustration.** From the Lewis perspective, the formation of a dative bond within H<sub>3</sub>B–NH<sub>3</sub> occurs when two electrons are donated by the nitrogen atom and accepted by boron.<sup>75</sup> This is known to be an oversimplification of the dative bond concept, where the strength of the donor does not necessarily match that of the acceptor. A mismatch in donor and acceptor strength endows the termini with a reduction or buildup of electron density, which we refer to as “frustration”. The frustrated termini utilize their immediate substituents to satisfy further electronic needs and provide a unique character of chemical bonding.

Frustration is quantified by examining the differences in charge changes between the bonded and the separated states. The atomic termini of the dative bond experience a change in atomic charge ( $Q_N(\text{dat})$  and  $Q_B(\text{dat})$ ) compared to their separated states ( $Q_N(\text{sep})$  and  $Q_B(\text{sep})$ ) by approximately equal but opposite amounts, where  $Q_N(\text{dat}) - Q_N(\text{sep}) \approx -[Q_B(\text{dat}) - Q_B(\text{sep})]$  or  $\Delta Q_N \approx -\Delta Q_B$ .<sup>75</sup> In other words, the donation (loss) of electron density from the donor ( $\Delta Q_N$ ) will be approximately equal in magnitude to the electron density accepted (gained) by the acceptor ( $\Delta Q_B$ ). Consequently, the extent in which  $\Delta Q_N$  equals  $-\Delta Q_B$  is used to gauge the dative character of a chemical bond. If  $\Delta Q_N$  equals  $-\Delta Q_B$ , then the B–N bond is considered fully dative, indicating no offset from equality, where a perfect match between donating and accepting electron density is achieved. If  $\Delta Q_N$  does not equal  $-\Delta Q_B$ , then the difference,  $Q_{\text{CTF}} = -(\Delta Q_B + \Delta Q_N)$ , represents the charge-transfer frustration, or mismatch of donor and acceptor strengths, between the



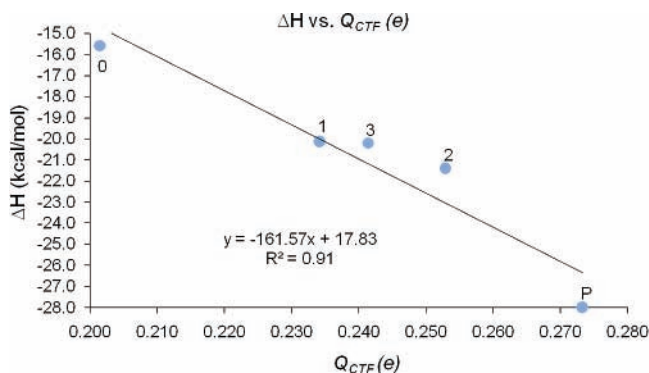


**Figure 6.** MP2 predicted binding enthalpy (BSSE and convergence corrections included) utilizing the 6-311++G(3df,2p) basis set for  $(\text{CH}_3)_3\text{B}-\text{N}(\text{CH}_3)_n\text{H}_{3-n}$ ,  $n = 0-3$ , and ammonia borane vs the charge-transfer frustration,  $Q_{\text{CTF}}$ , given by  $-(\Delta Q_{\text{B}} + \Delta Q_{\text{N}})$ . Labels near each data point refer to  $n$ , or number of methyl substitutions. P refers to the prototype dative bond,  $\text{H}_3\text{B}-\text{NH}_3$ .

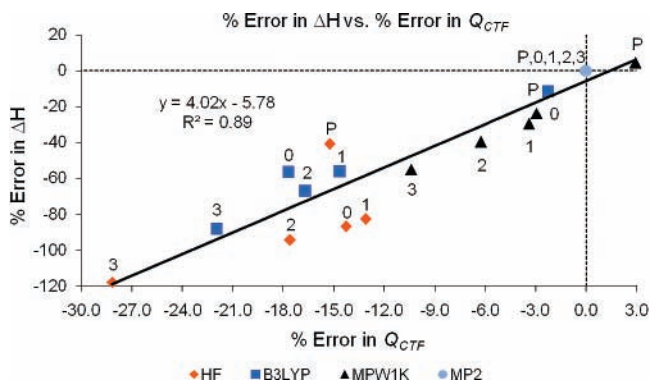


**Figure 7.** Percent error in the predicted binding enthalpy vs the percent error in the predicted charge-transfer frustration, given by  $-(\Delta Q_{\text{B}} + \Delta Q_{\text{N}})$  for HF (orange diamond), B3LYP (blue square), MPW1K (black triangle), and MP2 (gray circle) utilizing the 6-311++G(3df,2p) basis set on the corresponding optimized  $\text{H}_3\text{B}-\text{NH}_3$  and  $(\text{CH}_3)_3\text{B}-\text{N}(\text{CH}_3)_n\text{H}_{3-n}$ ,  $n = 0-3$ , structures or number of methyl substitution. Labels below or above each data point refer to  $n$ . P refers to the prototype dative bond,  $\text{H}_3\text{B}-\text{NH}_3$ .

two atoms. For example, MP2/6-311++G(3df,2p) predicts that  $\Delta Q_{\text{N}}$  and  $-\Delta Q_{\text{B}}$  are  $0.230e$  and  $0.503e$ , respectively, resulting in a  $Q_{\text{CTF}}$  of  $0.273e$ , which is considered to have relatively weak dative character in comparison to  $\text{F}_3\text{B}-\text{NH}_3$ , with a  $Q_{\text{CTF}}$  of  $0.000e$  computed at the same level of theory. This is in good agreement with the B3LYP/6-311++G(d,p) predicted value of  $-0.013e$  by Weinhold and Landis.<sup>75</sup> This suggests that  $\text{BF}_3$  is more compatible with  $\text{NH}_3$  than  $\text{BH}_3$ , which agrees with Pearson's Hard-Soft Acid-Base principles, because  $\text{BF}_3$  and  $\text{NH}_3$  are both hard and  $\text{BH}_3$  is soft.<sup>93,94</sup>

In addition, the B-N bond strength is stronger in  $\text{H}_3\text{B}-\text{NH}_3$  as compared to  $\text{F}_3\text{B}-\text{NH}_3$ .<sup>17,19</sup> Therefore, the relationship between the trend of binding enthalpies from methyl-substituted ammonia boranes and the extent of predicted charge-transfer frustration is of interest in characterizing the dative bond. Figure 6 displays the BSSE and convergence corrected MP2/6-311++G(3df,2p) predicted binding enthalpies versus  $Q_{\text{CTF}}$ . A strong linear correlation ( $R^2 = 0.91$ ) is found, suggesting that as the dative character of the bond increases, then the strength of the B-N bond decreases.

Figure 7 shows the percent error in the corrected predicted binding enthalpies for  $\text{H}_3\text{B}-\text{NH}_3$  and four trimethylboranes utilizing HF, B3LYP, MPW1K, and MP2 employing the 6-311++G(3df,2p) basis set versus the percent error in charge-transfer frustration between boron and nitrogen for each

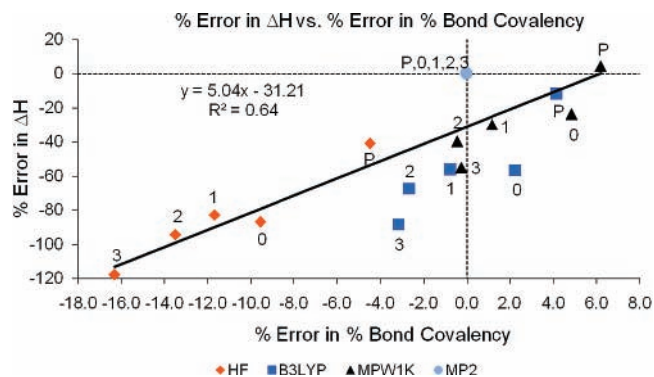


**Figure 8.** Percent error in the predicted binding enthalpy vs the percent error in the predicted percent bond covalency for HF (orange diamond), B3LYP (blue square), MPW1K (black triangle), and MP2 (gray circle) utilizing the 6-311++G(3df,2p) basis set on the corresponding optimized  $\text{H}_3\text{B}-\text{NH}_3$  and  $(\text{CH}_3)_3\text{B}-\text{N}(\text{CH}_3)_n\text{H}_{3-n}$ ,  $n = 0-3$ , structures or number of methyl substitution. Labels below or above each data point refer to  $n$ . P refers to the prototype dative bond,  $\text{H}_3\text{B}-\text{NH}_3$ .

corresponding method. A strong linear correlation ( $R^2 = 0.89$ ) exists, which suggests that modeling the dative character of the B-N bond is critical. Errors as large as 118% occur in the predicted binding enthalpy, if  $Q_{\text{CTF}}$  is underestimated by 28%, as predicted for  $(\text{CH}_3)_3\text{B}-\text{N}(\text{CH}_3)_3$  by HF. The charge-transfer frustrations predicted by MP2/6-311++G(3df,2p) between boron and nitrogen within  $\text{H}_3\text{B}-\text{NH}_3$ ,  $(\text{CH}_3)_3\text{B}-\text{NH}_3$ ,  $(\text{CH}_3)_3\text{B}-\text{NH}_2\text{CH}_3$ ,  $(\text{CH}_3)_3\text{B}-\text{N}(\text{CH}_3)_2$ , and  $(\text{CH}_3)_3\text{B}-\text{N}(\text{CH}_3)_3$  are  $0.273e$ ,  $0.202e$ ,  $0.234e$ ,  $0.253e$ , and  $0.241e$ , respectively. The  $Q_{\text{CTF}}$  trend across the dative bond with methyl substitution at either the donor or acceptor is rationalized by the electronegativities for nitrogen, carbon, hydrogen, and boron, which are 3.0, 2.5, 2.1, and 2.0, respectively.<sup>8</sup> Methyl substitution (comparing  $\text{H}_3\text{B}-\text{NH}_3$  and  $(\text{CH}_3)_3\text{B}-\text{NH}_3$ ) withdraws electron density from boron, due to the difference in electronegativities, resulting in a decrease of charge-transfer frustration and weakening of the B-N bond, as observed by experiment.<sup>26</sup> For the donor, increasing  $n$  within  $(\text{CH}_3)_3\text{B}-\text{N}(\text{CH}_3)_n\text{H}_{3-n}$  results in more donation of electron density to nitrogen, allowing nitrogen to become a stronger Lewis base. Thus, the charge-transfer frustration across the B-N bond increases from  $n = 0$  to  $n = 2$ , yielding a stronger B-N bond, except for when  $n = 3$ . However, steric congestion cannot be ignored in this system, and the balance of sterics and electronics is discussed later.

**Bond Covalency and Ionicity.** Although no strong correlation exists between bond order and binding enthalpy ( $R^2 = 0.50$ , Figure S5 of the Supporting Information), moderate correlations were found between the errors in binding enthalpy and both the errors in percent bond ionicity and percent bond covalency. Figure 8 displays a correlation ( $R^2 = 0.64$ ) between the percent error in binding enthalpy and the percent error in percent bond covalency. Large errors in the predicted binding enthalpy result from moderate errors in the percent bond covalency. For example, HF underestimates the percent bond covalency in the B-N dative bond within  $(\text{CH}_3)_3\text{B}-\text{N}(\text{CH}_3)_3$  by 16.3%, resulting in a predicted binding enthalpy of  $\Delta H_{373} = 3.6$  kcal/mol, a 118% underestimation from the BSSE and convergence corrected MP2 predicted value of  $-20.2$  kcal/mol. DFT and HF underestimate the binding enthalpy of the B-N bond for all systems, except for  $\text{H}_3\text{B}-\text{NH}_3$ , as predicted with MPW1K. The data support that the bond covalency must be predicted correctly to model an accurate binding enthalpy.

MP2/6-311++G(3df,2p) predicts the percent bond covalency for the dative bond between boron and nitrogen to decrease with increasing methyl substitutions within  $\text{H}_3\text{B}-\text{NH}_3$ ,  $(\text{CH}_3)_3\text{B}-$

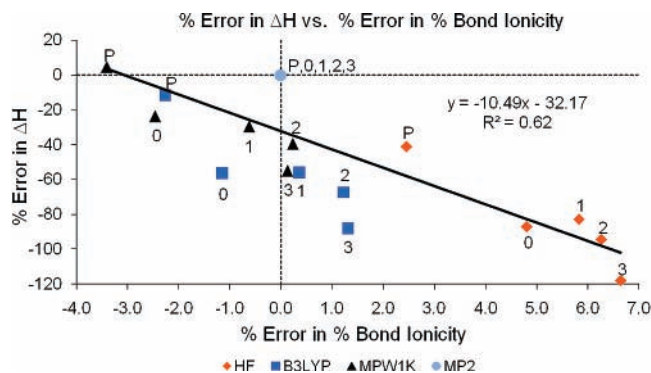


**Figure 9.** Percent error in the predicted binding enthalpy vs the percent error in the predicted percent bond ionicity for HF (orange diamond), B3LYP (blue square), MPW1K (black triangle), and MP2 (gray circle) utilizing the 6-311++G(3df,2p) basis set on the corresponding optimized  $\text{H}_3\text{B}-\text{NH}_3$  and  $(\text{CH}_3)_n\text{B}-\text{N}(\text{CH}_3)_m\text{H}_{3-n}$ ,  $n = 0-3$ , structures or number of methyl substitution. Labels below or above each data point refer to  $n$ . P refers to the prototype dative bond,  $\text{H}_3\text{B}-\text{NH}_3$ .

$\text{NH}_3$ ,  $(\text{CH}_3)_2\text{B}-\text{NH}_2\text{CH}_3$ ,  $(\text{CH}_3)_2\text{B}-\text{NH}(\text{CH}_3)_2$ , and  $(\text{CH}_3)_3\text{B}-\text{N}(\text{CH}_3)_3$  with values of 35.4%, 33.5%, 33.4%, 31.7%, and 28.9%, respectively. The data suggest that the covalency must be modeled correctly to predict an accurate binding enthalpy; however, it does not explain the trend in predicted or observed binding enthalpies, which is in agreement with Jonas et al.<sup>17</sup> Jonas and co-workers found that strong dative bonds may be primarily bound by either covalent or ionic interactions and that no correlation exists between the strength of the bond and the degree of covalency or ionicity.<sup>17</sup> A balance of electronics and steric factors must be considered in such crowded systems, as discussed in a later section.

A correlation ( $R^2 = 0.62$ ) also exists between errors in percent bond ionicity and binding enthalpy, as shown in Figure 9. HF overestimates the percent bond ionicity, which results in weaker predicted binding enthalpies compared to MP2. In addition, B3LYP and MPW1K result in weaker binding enthalpies, except for  $\text{H}_3\text{B}-\text{NH}_3$ , as predicted by MPW1K. As with the error in covalency, moderate errors in ionicity yield large errors in the binding enthalpy. For example, an error of 6.7% in percent ionicity results in a 118% error in binding enthalpy. The data support that the percent bond ionicity must be predicted correctly to predict an accurate binding enthalpy. MP2/6-311++G(3df,2p) predicts the percent bond ionicity for the dative bond between boron and nitrogen to increase with increasing methyl substitutions within  $\text{H}_3\text{B}-\text{NH}_3$ ,  $(\text{CH}_3)_2\text{B}-\text{NH}_3$ ,  $(\text{CH}_3)_2\text{B}-\text{NH}_2\text{CH}_3$ ,  $(\text{CH}_3)_2\text{B}-\text{NH}(\text{CH}_3)_2$ , and  $(\text{CH}_3)_3\text{B}-\text{N}(\text{CH}_3)_3$ , with percentages of 64.6%, 66.5%, 66.6%, 68.3%, and 71.1%, respectively. The ionicity increases by approximately the same amount as the decrease in covalency with methyl substitution. As discussed with the covalency, the extent to which the bond is ionic does not explain the binding enthalpy trend. The percent error in binding enthalpy is more sensitive to the percent error in ionic character over covalent character as indicated by the magnitude of the slope of the fitted line displayed in Figures 8 and 9 (10.5 vs 5.0). The data suggest that the ionic nature of the wave function is more difficult to model than the covalent character.

**Balance of Steric and Electronic Effects.** The charge-transfer frustration at equilibrium is crucial to characterizing the nature of the dative bond and subsequently predicting accurate binding enthalpies. However, from the previous discussion, the predicted dative bond descriptors do not fully explain the reported experimental trend for  $n = 2$  to  $n = 3$ . The MP2/6-311++G(3df,2p) predicted binding enthalpies (with BSSE and convergence corrections) versus  $Q_{\text{CTF}}$  display a strong linear

correlation ( $R^2 = 0.91$ ), implying the nature of the dative bond has consequences on the binding enthalpy. However, the reason for why the binding enthalpy decreases and the dative character has increased upon methyl substitution ( $n = 2$  to  $n = 3$ ) is not revealed by analyzing the dative bond descriptors. A balance of sterics and electronics must be considered.

In an analysis of the predicted geometries, it is found that the atomic termini of the dative bond allow for the substituted groups to relieve steric strain by the bending of angles. The acceptor's tetrahedral geometry is rigid compared to the donor's. The predicted acceptor XBN angles ( $X = \text{H}$  or  $\text{C}$ ) vary only by  $3.1^\circ$ , whereas the donor XNB angles vary by  $14.2^\circ$ , depending upon the number of methyl substitutions. As methyl groups are added to the donor, steric congestion is relieved by expanding the CNB angles with a corresponding angle compression of  $\angle\text{HNB}$  for  $n = 1$  and  $n = 2$ . The donor group appears to "rotate" to relieve the steric congestion away from the three methyl groups on the acceptor. For example, when one methyl is added ( $n = 1$ ), the CNB angle becomes  $117.2^\circ$  ( $6.4^\circ$  greater than  $\angle\text{HNB}$  when  $n = 0$ ), while the HNB angles compress to  $106.7^\circ$  ( $4.1^\circ$  less than  $\angle\text{HNB}$  when  $n = 0$ ). With the combined relief of steric strain and the donation of electron density by the methyl group, the computed B-N bond is strengthened and shortens by  $0.005 \text{ \AA}$ . The result is an experimentally observed energy lowering of  $3.8 \text{ kcal/mol}$ , compared to when  $n = 0$ . When two methyl groups are added, the CNB angles become  $114.0^\circ$  ( $3.2^\circ$  greater than  $\angle\text{HNB}$  where  $n = 0$ ) with a corresponding HNB angle of  $103.0^\circ$  ( $7.8^\circ$  less than  $\angle\text{HNB}$  where  $n = 0$ ). There is less rotation of the methyl groups for steric relief; however, the two methyl groups donate electron density to nitrogen, decreasing the dative character of the B-N bond (Figure 6). Consequently, the combined effect is a  $1.7 \text{ kcal/mol}$  stabilization observed experimentally. Finally, addition of the last methyl group cannot utilize the rotation mechanism for stabilization due to the symmetric nature of the substitution. When  $n = 3$  the CNB angle is found to be nearly tetrahedral at  $110.9^\circ$ , contracting by only  $0.1^\circ$  when  $n = 0$ . Despite the electron donation by three methyl groups, the lack of steric relief by rotation prevents potential stabilization. Consequently, a destabilization of  $3.4 \text{ kcal/mol}$  with a B-N bond elongation of  $0.027 \text{ \AA}$  from  $n = 0$  occurs, decreasing the charge-transfer frustration and subsequently increasing the dative character. The B-N destabilization and corresponding  $Q_{\text{CTF}}$  decrease are observed within Figure 6, correlating well with the remaining ammonia borane data. In summary, the data suggest that methyl substitution stabilizes the B-N bond by decreasing the dative nature. The bond is further stabilized by relieving steric congestion by geometric distortion. Subsequent methyl substitutions become increasingly crowded and difficult to accommodate despite the stabilization offered by reducing the dative nature of the bond. In addition, N-C and B-C elongations participate very little in the relief of steric congestion, if at all, because only  $0.003$  and  $0.007 \text{ \AA}$  variations are predicted across the methylated ammonia boranes, respectively.

## Conclusion

The importance of a balance of electronic and steric factors at the equilibrium distance is shown to be critical in modeling and characterizing the dative bond. Discrepancies in the binding energetics reported within the literature are not a consequence of varying dative bond length but rather of how the specific method and basis set model the electronics within the system. More specifically, the charge-transfer frustration between boron and nitrogen must be predicted correctly to model the B-N

dative bond accurately. The binding enthalpy trend is a consequence of the dative character of the bond, which is measured by the completeness of charge transfer, or to what extent  $\Delta Q_N$  equals  $-\Delta Q_B$ . In this particular system, steric forces cannot be ignored. The Lewis donor has been found to be more flexible than the acceptor, allowing steric congestion to be relieved for the addition of two methyl groups. However, addition of the final methyl group results in severe steric congestion ( $n = 3$ ), and the binding enthalpy weakens, because the molecule can no longer distort to lower its energy. It is recommended that if accurate binding enthalpies are desired on a quantitative level (MAD of 0.5 kcal/mol), then single-point energy calculations utilizing QCISD(T)/6-311++G(3df,2p) should be utilized, incorporating BSSE corrections with the 1.6 kcal/mol convergence correction on MP2/6-311++G(3df,2p) optimized structures as well as appropriate thermal corrections to the electronic energy. However, if semiquantitative results are desired (MAD of 2.2 kcal/mol), maintaining the qualitative trend, then full optimizations utilizing MP2/6-311++G(3df,2p) should be employed, incorporating BSSE corrections with the 1.5 kcal/mol convergence correction and appropriate thermal corrections. MP2 utilized with the 6-311++G(3df,2p) basis set offers an appropriate balance of accuracy and efficiency to model the energetics of larger B–N dative bond systems. B3LYP was successful and MPW1K unsuccessful at modeling the bond length for ammonia borane. Furthermore, all DFT methods did not model experimental binding enthalpies and trends for the four methyl-substituted ammonia trimethylboranes ((CH<sub>3</sub>)<sub>3</sub>B–N(CH<sub>3</sub>)<sub>n</sub>H<sub>3–n</sub>;  $n = 0–3$ ) accurately. Proper treatment of the dative bond allowed for an interpretation of the experimental binding enthalpies for the methyl-substituted ammonia trimethylboranes. In summary, this study provides a comprehensive evaluation of computational protocols used in the study of dative bonds. However, it is suspected that weaker Lewis acid–base adducts or stronger organometallic compounds may have different sensitivity and response to the computational factors studied here. Ongoing work in both fields will be reported soon to provide a fuller and more robust understanding across a range of dative bonding.

**Acknowledgment.** This work was funded in part by the National Science Foundation and Department of Defense (Grant Nos. CHE-0723109, CHE-0649182, CHE-0321147, CHE-0354052, and AAB/PSC CHE-030008P), Department of Education (Grant Nos. P116Z040100 and P116Z050331), and the Silicon Graphics Inc., James River Technical, Inc., and Gaussian Corporations. The authors acknowledge Dr. Roberto Gomperts (SGI) for his expertise and for providing the necessary resources to perform a QCISD(T)/6-311++G(3df,2p)//MP2/6-311++G(3df,2p) single-point energy computation incorporating BSSE corrections on (CH<sub>3</sub>)<sub>3</sub>B–N(CH<sub>3</sub>)<sub>3</sub>. In addition, the expertise, knowledge, and discussions with Dr. Doug Fox (Gaussian) were crucial to this study.

**Supporting Information Available:** All optimized structures, single points, BSSE corrections, frequencies, thermodynamic data, figures displaying Haaland's estimation, interpolation of the scaling factor at 373 K, convergence of B–N bond lengths and BSSE corrected binding enthalpies for H<sub>3</sub>B–NH<sub>3</sub> for remaining basis sets, percent error in binding enthalpy versus percent error in bond order, tables displaying all B–N bond lengths, BSSE uncorrected corrected binding enthalpies, and amount of BSSE incorporated with each level of theory. This material is free of charge via the Internet at <http://pubs.acs.org>.

## References and Notes

- (1) Glaser, R.; Knotts, N. *J. Phys. Chem. A* **2006**, *110*, 1295.
- (2) Fiorillo, A. A.; Galbraith, J. M. *J. Phys. Chem. A* **2004**, *108*, 5126.
- (3) Haaland, A. *Angew. Chem.* **1989**, *101*, 1017.
- (4) Linton, E. P. *J. Am. Chem. Soc.* **1940**, *62*, 1945.
- (5) Wittig, G. *Angew. Chem.* **1951**, *63*, 15.
- (6) Chatt, J. *Nature* **1950**, *165*, 637.
- (7) Chatt, J.; Hitchcock, P. B.; Pidcock, A.; Warrens, C. P.; Dixon, K. R. *J. Chem. Soc., Dalton Trans.* **1984**, 2237.
- (8) Pauling, L. C. *The Nature of the Chemical Bond and the Structure of Molecules and Crystals; An Introduction to Modern Structural Chemistry*, 3rd ed; Cornell University Press: Ithaca, NY, 1960.
- (9) Gillespie, R. J.; Robinson, E. A. *J. Comput. Chem.* **2007**, *28*, 87.
- (10) Shaik, S. *J. Comput. Chem.* **2007**, *28*, 51.
- (11) *Classics in Coordination Chemistry: The Selected Papers of Alfred Werner*; Kauffman, G. B., Ed.; Classics of Science 4; Dover Publications: New York, 1968.
- (12) Jensen, W. B. *The Lewis Acid–Base Concepts: An Overview*; Wiley: New York, 1980.
- (13) Gur'yanova, E. N.; Gol'dshtein, I. P.; Romm, I. P. *Donor–acceptor Bond*; Wiley: New York, 1975.
- (14) *Hard and Soft Acids and Bases*; Pearson, R. G., Ed.; Benchmark Papers in Inorganic Chemistry; Dowden, Hutchinson & Ross: Stroudsburg, PA, 1973.
- (15) Gutmann, V. *The Donor–Acceptor Approach to Molecular Interactions*; Plenum Press: New York, 1978.
- (16) Zhong, D.; Zewail, A. H. *Proc. Natl. Acad. Sci. U.S.A.* **1999**, *96*, 2602.
- (17) Jonas, V.; Frenking, G.; Reetz, M. T. *J. Am. Chem. Soc.* **1994**, *116*, 8741.
- (18) Anane, H.; Boutalib, A.; Nebot-Gil, I.; Francisco, T. *Chem. Phys. Lett.* **1998**, *287*, 575.
- (19) Bauschlicher, C. W., Jr.; Ricca, A. *Chem. Phys. Lett.* **1995**, *237*, 14.
- (20) Gilbert, T. M. *J. Phys. Chem. A* **2004**, *108*, 2550.
- (21) LeTourneau, H. A.; Birsch, R. E.; Korbeck, G.; Radkiewicz-Poutsma, J. L. *J. Phys. Chem. A* **2005**, *109*, 12014.
- (22) Jagielska, A.; Moszynski, R.; Piela, L. *J. Chem. Phys.* **1999**, *110*, 947.
- (23) Rayon, V. M.; Sordo, J. A. *J. Mol. Struct.: THEOCHEM* **1998**, *426*, 171.
- (24) Anane, H.; Boutalib, A.; Nebot-Gil, I.; Tomas, F. *J. Phys. Chem. A* **1998**, *102*, 7070.
- (25) Umeyama, H.; Morokuma, K. *J. Am. Chem. Soc.* **1976**, *98*, 7208.
- (26) Brown, H. C.; Bartholomay, H., Jr.; Taylor, M. D. *J. Am. Chem. Soc.* **1944**, *66*, 435.
- (27) *Thermodynamic Properties of Individual Substances*, 4th ed.; Gurvich, L. V., Veyts, I. V., Alcock, C. B., Eds.; Hemisphere Publishing: New York, 1994; Vol. 3.
- (28) Allendorf, M. D.; Melius, C. F. *J. Phys. Chem. A* **1997**, *101*, 2670.
- (29) Anane, H.; El Houssame, S.; El Guerraze, A.; Jarid, A.; Boutalib, A.; Nebot-Gil, I.; Tomas, F. *J. Mol. Struct.: THEOCHEM* **2004**, *709*, 103.
- (30) Bhat, K. L.; Howard, N. J.; Rostami, H.; Lai, J. H.; Bock, C. W. *J. Mol. Struct.: THEOCHEM* **2005**, *723*, 147.
- (31) Gutowski, K. E.; Dixon, D. A. *J. Phys. Chem. A* **2006**, *110*, 8840.
- (32) Grant, D. J.; Dixon, D. A. *J. Phys. Chem. A* **2005**, *109*, 10138.
- (33) Nxumalo, L. M.; Andrzejak, M.; Ford, T. A. *J. Chem. Inf. Comput. Sci.* **1996**, *36*, 377.
- (34) Dixon, D. A.; Gutowski, M. *J. Phys. Chem. A* **2005**, *109*, 5129.
- (35) Nguyen, M. T.; Nguyen, V. S.; Matus, M. H.; Gopakumar, G.; Dixon, D. A. *J. Phys. Chem. A* **2007**, *111*, 679.
- (36) Haubner, R.; Wilhelm, M.; Weissenbacher, R.; Lux, B. *Struct. Bonding* **2002**, *102*, 1.
- (37) Karim, M. Z.; Cameron, D. C.; Murphy, M. J.; Hashmi, M. S. J. *Proc. Inst. Mech. Eng., IMechE Conf.* **1991**, 181.
- (38) Einset, E. O.; Patibandla, N.-B.; Luthra, K. L. *J. Am. Ceram. Soc.* **1994**, *77*, 3081.
- (39) Lii, D.-F.; Huang, J.-L.; Tsui, L.-J.; Lee, S.-M. *Surf. Coat. Technol.* **2002**, *150*, 269.
- (40) Huang, J. L.; Pan, C. H.; Lii, D. F. *Surf. Coat. Technol.* **1999**, *122*, 166.
- (41) Hall, I. H.; Spielvogel, B. F.; Sood, A. *Anti-Cancer Drugs* **1990**, *1*, 133.
- (42) Fisher, L.; Holme, T. *J. Comput. Chem.* **2001**, *22*, 913.
- (43) Burnham, B. S. *Curr. Med. Chem.* **2005**, *12*, 1995.
- (44) Sood, A.; Sood, C. K.; Spielvogel, B. F.; Hall, I. H.; Wong, O. T. *J. Pharm. Sci.* **1992**, *81*, 458.
- (45) Clementi, E.; Meldolesi, J. *Cell Calcium* **1996**, *19*, 269.
- (46) Gibson, A.; Fernandes, F.; Wallace, P.; McFadzean, I. *Br. J. Pharmacol.* **2001**, *134*, 233.
- (47) Putney, J. W., Jr. *Mol. Interventions* **2001**, *1*, 84.

- (48) Frisch, M. J.; Trucks, G. W.; Schlegel, H. B.; Scuseria, G. E.; Robb, M. A.; Cheeseman, J. R.; Montgomery, J. A., Jr.; Vreven, T.; Kudin, K. N.; Burant, J. C.; Millam, J. M.; Iyengar, S. S.; Tomasi, J.; Barone, V.; Mennucci, B.; Cossi, M.; Scalmani, G.; Rega, N.; Petersson, G. A.; Nakatsuji, H.; Hada, M.; Ehara, M.; Toyota, K.; Fukuda, R.; Hasegawa, J.; Ishida, M.; Nakajima, T.; Honda, Y.; Kitao, O.; Nakai, H.; Klene, M.; Li, X.; Knox, J. E.; Hratchian, H. P.; Cross, J. B.; Bakken, V.; Adamo, C.; Jaramillo, J.; Gomperts, R.; Stratmann, R. E.; Yazyev, O.; Austin, A. J.; Cammi, R.; Pomelli, C.; Ochterski, J. W.; Ayala, P. Y.; Morokuma, K.; Voth, G. A.; Salvador, P.; Dannenberg, J. J.; Zakrzewski, V. G.; Dapprich, S.; Daniels, A. D.; Strain, M. C.; Farkas, O.; Malick, D. K.; Rabuck, A. D.; Raghavachari, K.; Foresman, J. B.; Ortiz, J. V.; Cui, Q.; Baboul, A. G.; Clifford, S.; Cioslowski, J.; Stefanov, B. B.; Liu, G.; Liashenko, A.; Piskorz, P.; Komaromi, I.; Martin, R. L.; Fox, D. J.; Keith, T.; Al-Laham, M. A.; Peng, C. Y.; Nanayakkara, A.; Challacombe, M.; Gill, P. M. W.; Johnson, B.; Chen, W.; Wong, M. W.; Gonzalez, C.; Pople, J. A. *Gaussian 03*, revision D.01; Gaussian, Inc.: Wallingford, CT, 2004.
- (49) Møller, C.; Plesset, M. S. *Phys. Rev.* **1934**, *46*, 618.
- (50) Head-Gordon, M.; Head-Gordon, T. *Chem. Phys. Lett.* **1994**, *220*, 122.
- (51) Gauss, J.; Cremer, D. *Chem. Phys. Lett.* **1988**, *150*, 280.
- (52) Pople, J. A.; Head-Gordon, M.; Raghavachari, K. *J. Chem. Phys.* **1987**, *87*, 5968.
- (53) Becke, A. D. *J. Chem. Phys.* **1993**, *98*, 5648.
- (54) Lee, C.; Yang, W.; Parr, R. G. *Phys. Rev.* **1988**, *37*, 785.
- (55) Lynch, B. J.; Fast, P. L.; Harris, M.; Truhlar, D. G. *J. Phys. Chem. A* **2000**, *104*, 4811.
- (56) Hehre, W. J.; Ditchfield, R.; Pople, J. A. *J. Chem. Phys.* **1972**, *56*, 2257.
- (57) Frisch, M. J.; Pople, J. A.; Binkley, J. S. *J. Chem. Phys.* **1984**, *80*, 3265.
- (58) Krishnan, R.; Binkley, J. S.; Seeger, R.; Pople, J. A. *J. Chem. Phys.* **1980**, *72*, 650.
- (59) Binkley, J. S.; Pople, J. A.; Hehre, W. J. *J. Am. Chem. Soc.* **1980**, *102*, 939.
- (60) Ditchfield, R.; Hehre, W. J.; Pople, J. A. *J. Chem. Phys.* **1971**, *54*, 724.
- (61) Hehre, W. J.; Stewart, R. F.; Pople, J. A. *J. Chem. Phys.* **1969**, *51*, 2657.
- (62) Hariharan, P. C.; Pople, J. A. *Theor. Chim. Acta* **1973**, *28*, 213.
- (63) Woon, D. E.; Dunning, T. H., Jr. *J. Chem. Phys.* **1993**, *98*, 1358.
- (64) Dunning, T. H., Jr. *J. Chem. Phys.* **1989**, *90*, 1007.
- (65) Woon, D. E.; Dunning, T. H., Jr. *J. Chem. Phys.* **1994**, *100*, 2975.
- (66) Kendall, R. A.; Dunning, T. H., Jr.; Harrison, R. J. *J. Chem. Phys.* **1992**, *96*, 6796.
- (67) Scott, A. P.; Radom, L. *J. Phys. Chem.* **1996**, *100*, 16502.
- (68) Giesen, D. J.; Phillips, J. A. *J. Phys. Chem. A* **2003**, *107*, 4009.
- (69) Davidson, E. R.; Feller, D. *Chem. Rev.* **1986**, *86*, 681.
- (70) Gutowski, M.; Van Duijneveldt, F. B.; Chalasinski, G.; Piela, L. *Mol. Phys.* **1987**, *61*, 233.
- (71) Gutowski, M.; Van Duijneveldt, F. B.; Chalasinski, G.; Piela, L. *Chem. Phys. Lett.* **1986**, *129*, 325.
- (72) Gutowski, M.; Chalasinski, G. *J. Chem. Phys.* **1993**, *98*, 5540.
- (73) Kestner, N. R.; Combariza, J. E. *Rev. Comput. Chem.* **1999**, *13*, 99.
- (74) Boys, S. F.; Bernardi, F. *Mol. Phys.* **1970**, *19*, 553.
- (75) Weinhold, F.; Landis, C. *Valency and Bonding: A Natural Bond Orbital Donor–Acceptor Perspective*; Cambridge University Press: Cambridge, U. K., 2005.
- (76) Glendening, E. D.; Badenhop, J. K.; Reed, A. E.; Carpenter, J. E.; Bohmann, J. A.; Morales, C. M.; Weinhold, F. *NBO 5.0*; Theoretical Chemistry Institute, University of Wisconsin: Madison, WI, 2001. <http://www.chem.wisc.edu/~nbo5>.
- (77) Reed, A. E.; Weinstock, R. B.; Weinhold, F. *J. Chem. Phys.* **1985**, *83*, 735.
- (78) Gross, K. C.; Seybold, P. G.; Hadad, C. M. *Int. J. Quantum Chem.* **2002**, *90*, 445.
- (79) Clark, A. E.; Sonnenberg, J. L.; Hay, P. J.; Martin, R. L. *J. Chem. Phys.* **2004**, *121*, 2563.
- (80) Bultinck, P.; Langenaeker, W.; Lahorte, P.; De Proft, F.; Geerlings, P.; Van Alsenoy, C.; Tollenaere, J. P. *J. Phys. Chem. A* **2002**, *106*, 7895.
- (81) Glendening, E. D.; Badenhop, J. K.; Weinhold, F. *J. Comput. Chem.* **1998**, *19*, 628.
- (82) Glendening, E. D.; Weinhold, F. *J. Comput. Chem.* **1998**, *19*, 610.
- (83) Glendening, E. D.; Weinhold, F. *J. Comput. Chem.* **1998**, *19*, 593.
- (84) Thorne, L. R.; Suenram, R. D.; Lovas, F. J. *J. Chem. Phys.* **1983**, *78*, 167.
- (85) Suenram, R. D.; Thorne, L. R. *Chem. Phys. Lett.* **1981**, *78*, 157.
- (86) Helgaker, T.; Ruden, T. A.; Jorgensen, P.; Olsen, J.; Klopper, W. *J. Phys. Org. Chem.* **2004**, *17*, 913.
- (87) Feller, D.; Peterson, K. A. *J. Chem. Phys.* **2007**, *126*, 114105.
- (88) Feller, D.; Peterson, K. A. *J. Chem. Phys.* **1998**, *108*, 154.
- (89) Woon, D. E. *Chem. Phys. Lett.* **1993**, *204*, 29.
- (90) Dunning, T. H., Jr. *J. Phys. Chem. A* **2000**, *104*, 9062.
- (91) Peterson, K. A.; Kendall, R. A.; Dunning, T. H., Jr. *J. Chem. Phys.* **1993**, *99*, 9790.
- (92) Curtiss, L. A.; Redfern, P. C.; Raghavachari, K. *J. Chem. Phys.* **2007**, *126*, 084108.
- (93) Pearson, R. G. *J. Chem. Educ.* **1968**, *45*, 643.
- (94) Pearson, R. G. *J. Chem. Educ.* **1968**, *45*, 581.